An Investigation of $\pi-\pi$ Packing in a Columnar Hexabenzocoronene by Fast Magic-Angle Spinning and Double-Quantum ^{1}H Solid-State NMR Spectroscopy

Steven P. Brown, Ingo Schnell, Johann Diedrich Brand, Klaus Müllen, and Hans Wolfgang Spiess*

Max-Planck-Institut für Polymerforschung, Postfach 3148, D-55021 Mainz, Germany

Received March 1, 1999. Revised Manuscript Received May 10, 1999

Abstract: ^{1}H NMR methods employing very fast magic-angle spinning (MAS) are applied to the investigation of both the structure and dynamics of an alkyl-substituted hexa-*peri*-hexabenzocoronene (HBC), which is known to form a columnar mesophase with a very high one-dimensional charge carrier mobility. For the crystalline phase, three distinct aromatic resonances are identified in the single-quantum MAS spectrum. The observation of these distinct aromatic resonances is explained in terms of the differing degrees to which the aromatic protons experience the ring current of adjacent layers. Using the rotor-synchronized double-quantum MAS method, definite proton−proton proximities are identified, which are shown to be in agreement with the known crystal structure of unsubstituted HBC. In the liquid-crystalline phase, axial motion of the HBC disks leads to the averaging of the three sites into a single resonance. Furthermore, the reduction of the dipolar coupling caused by this motion is quantitatively investigated by an analysis of double-quantum MAS spinning sideband patterns. For all spectra, the resolution is significantly improved for a compound where the α-carbon positions have been deuterated; the synthesis of this deuterated compound, in particular the final cyclodehydrogenation step, is described.

Introduction

Solution-state ^{1}H NMR spectroscopy has established itself as an indispensable method for the investigation of structure and dynamics over a very wide range of applications.[1] However, for rigid solids, the application of ^{1}H NMR spectroscopy is complicated by the strong homonuclear proton−proton dipolar interaction;[2−4] this leads to substantial homogeneous broadening of the resonances, which is only partially narrowed by magic-angle spinning (MAS), such that chemical shift information is usually obscured. As a consequence, the routine use of solid-state NMR has, to date, focused on nuclei for which the dipolar interactions are weaker, such as ^{13}C and ^{2}H.

Over the past decade, much progress has been made in the area of fast MAS,[5] and probes capable of a rotation frequency, $\omega_R/2\pi$, of 35 kHz are now commercially available. Recently, we have shown that the resolution afforded by such a fast ω_R is sufficient to allow specific structural information to be obtained for organic solids by ^{1}H MAS NMR.[6] In particular, the information about the through-space proximity of dipolar-coupled nuclei provided by ^{1}H double-quantum (DQ) MAS spectroscopy[7−12] enabled specific information about hydrogen-bonding arrangements to be deduced. In this way, the DQ MAS method can be considered to be the analogue of the solution-state NOESY[1] experiment, the latter being heavily exploited in the structural elucidation of biopolymers.[13]

Another important intermolecular aspect which governs the mutual arrangement of molecules in condensed phases is the $\pi-\pi$ interaction, in particular that between aromatic moieties.[14] There is currently much interest in polycyclic aromatic materials, which form columnar mesophases, on account of, for example, their potential applications as vectorial charge transport layers in xerography, electrophotography, or molecular electronic devices. One such class of materials are the hexaalkyl-substituted hexa-*peri*-hexabenzocoronenes, an example of which has recently been shown to possess an exceptionally high one-dimensional charge carrier mobility.[15]

In this paper, we then apply ^{1}H MAS and ^{1}H DQ MAS NMR to the investigation of the structure and dynamics of hexa-*n*-

* To whom correspondence should be addressed.

(1) Ernst, R. R.; Bodenhausen, G.; Wokaun, A. *Principles of Nuclear Magnetic Resonance in One and Two Dimensions*; Clarendon: Oxford, 1987.

(2) Abragam, A. *The Principles of Nuclear Magnetism*; Clarendon: Oxford, 1961.

(3) Mehring, M. *Principles of High Resolution NMR in Solids*; Springer: Berlin, 1983.

(4) Schmidt-Rohr, K.; Spiess, H. W. *Multidimensional Solid State NMR and Polymers*; Academic Press: New York, 1994.

(5) Jakobson, H. J. *Encyclopedia of Nuclear Magnetic Resonance*; Wiley: Chichester, 1996; Vol. 1, p 398.

(6) Schnell, I.; Brown, S. P.; Low, H. Y.; Ishida, H.; Spiess, H. W. *J. Am. Chem. Soc.* **1998**, *120*, 11784.

(7) Geen, H.; Titman, J. J.; Gottwald, J.; Spiess, H. W. *Chem. Phys. Lett.* **1994**, *227*, 79.

(8) Sommer, W.; Gottwald, J.; Demco, D. E.; Spiess, H. W. *J. Magn. Reson.* **1995**, *A113*, 131.

(9) Geen, H.; Titman, J. J.; Gottwald, J.; Spiess, H. W. *J. Magn. Reson.* **1995**, *A 114*, 264.

(10) Gottwald, J.; Demco, D. E.; Graf, R.; Spiess, H. W. *Chem. Phys. Lett.* **1995**, *243*, 314.

(11) Feike, M.; Graf, R.; Schnell, I.; Jäger, C.; Spiess, H. W. *J. Am. Chem. Soc.* **1996**, *118*, 9631.

(12) Graf, R.; Demco, D. E.; Gottwald, J.; Hafner, S.; Spiess, H. W. *J. Chem. Phys.* **1997**, *106*, 885.

(13) Wüthrich, K. *NMR of Proteins and Nucleic Acids*; Wiley: New York, 1986.

(14) Desiraju, G. R. *Crystal Engineering: The Design of Organic Solids*; Elsevier: Amsterdam, 1989.

(15) Van de Craats, A. M.; Warman, J. M.; Müllen, K.; Geerts, Y.; Brand, J. D. *Adv. Mater.* **1998**, *10*, 36.

10.1021/ja990637m CCC: $18.00
Published on Web 06/25/1999

dodecyl-hexa-*peri*-hexabenzocoronene (henceforth referred to as HBC-C_{12}). This sample is known to form a remarkably stable columnar mesophase,[16] indicating strong $\pi-\pi$ packing, and has been previously studied by variable-temperature ^{2}H NMR spectra.[16] In addition, a STM image of a HBC-C_{12} monolayer adsorbed onto graphite,[17] as well as solution-state absorption and fluorescence spectra,[18] has been presented.

HBC-C_{12} samples with the α-carbons of the alkyl side chains either deuterated (87%, **1**; henceforth referred to as α-deuterated) or simply protonated (**2**) were prepared and investigated. In addition to providing structural information, high-resolution ^{1}H MAS NMR can also be used to study molecular dynamics. This is demonstrated by recording one- and two-dimensional spectra of HBC-C_{12} in both its solid and liquid-crystalline (LC) phases. The dynamical information so obtained is compared with the results of the previous investigation, where variable-temperature ^{2}H NMR spectra were recorded for a sample in which the aromatic hydrogens were deuterated.[16]

1 : R = D

2 : R = H

^{1}H NMR Investigation

One-Dimensional MAS Spectra. Figure 1 presents ^{1}H MAS spectra of the crystalline phases of (a) α-deuterated and (b) fully protonated HBC-C_{12}, as well as (c) the LC phase of α-deuterated HBC-C_{12}, recorded (in all cases) at an $\omega_R/2\pi$ of 35 kHz. For comparison, a solution-state spectrum of α-deuterated HBC-C_{12} is shown in Figure 1d. The six-fold symmetry of the individual molecules means that only one distinct aromatic proton resonance is expected, as is indeed observed to be the case in the solution-state spectrum. However, in Figure 1a, three aromatic resonances are clearly resolved; the effect of additional dipolar couplings to the α-carbon protons means that the three peaks are less well resolved in Figure 1b. Using data processing methods known from solution-state NMR, it is possible to enhance the resolution in the aromatic region. As an example of what can be achieved, the dashed line in Figure 1b shows the result of applying a method reported by Traficante and Nemeth.[19] We would, however, like to emphasize that such methods should be used with extreme care in solid-state NMR, since artifacts are often introduced, which cannot be distinguished from the genuine peaks.

On heating of the sample above the melting point, the three peaks transform into a single peak, with a line width which is significantly greater than that observed for an unordered melt (cf. Figure 3 of ref 6). It is also apparent that the chemical shift of the single aromatic peak in Figure 1d is significantly shifted to low field compared to that in Figure 1c (8.2 compared to 6.2 ppm). In this context, it is further interesting to note that the solution-state aromatic chemical shift was observed to shift to low field on decreasing the concentration, ranging from 8.0 ppm at a concentration of 0.017 M to 8.9 ppm at 1.7×10^{-6} M.

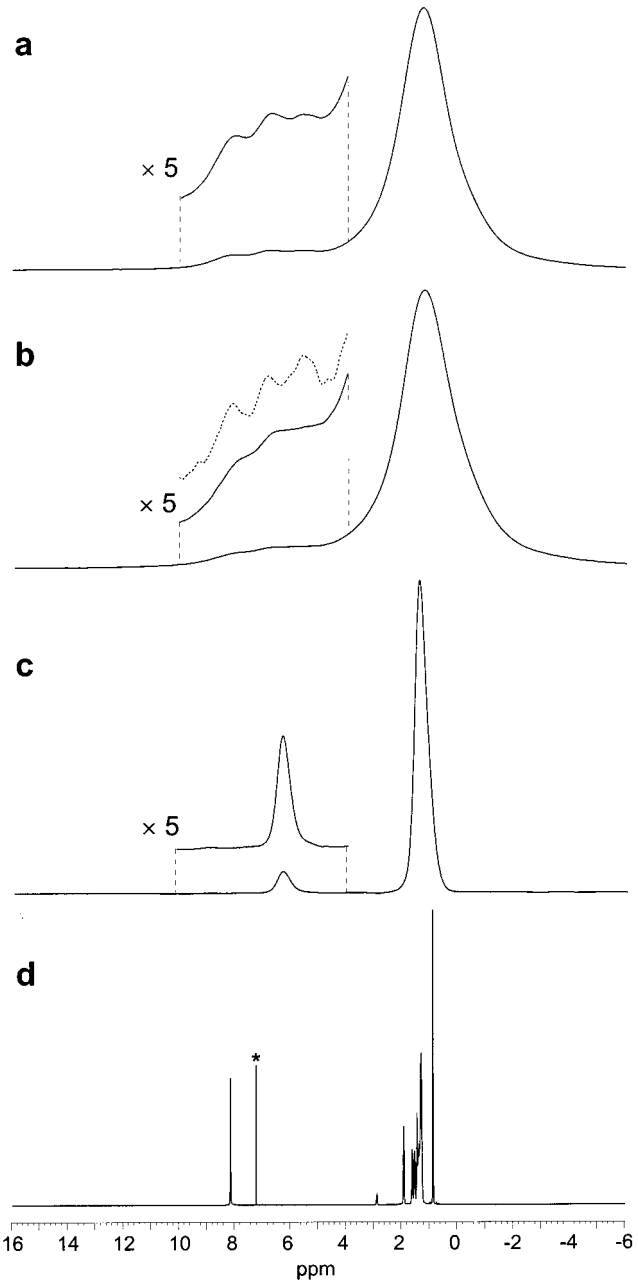

Figure 1. One-dimensional ^{1}H NMR spectra of (a, c, d) α-deuterated and (b) fully protonated HBC-C_{12} in different physical states, namely (a, b) the crystalline phase at 333 K, (c) the LC phase at 383 K, and (d) dissolved in deuterated chloroform. The spectra a−c were recorded under MAS at 35 kHz. The dashed line in spectrum b shows the enhanced resolution achieved by a data processing method reported by Traficante and Nemeth.[19] The asterisk in spectrum d indicates the signal due to residual $CHCl_3$.

In principle, the observed changes in the ^{1}H MAS spectra can be ascribed to two different scenarios: either there exist three different types of HBC crystallographic environment, where the six-fold symmetry of each individual molecule is *maintained*, with the three environments then becoming equivalent in the LC phase; or there is a *reduction* of the six-fold symmetry of each molecule due to the packing arrangement in

(16) Herwig, P.; Kayser, C. W.; Müllen, K.; Spiess, H. W. *Adv. Mater.* **1996**, *8*, 510.
(17) Stabel, A.; Herwig, P.; Müllen, K.; Rabe, J. P. *Angew. Chem., Int. Ed. Engl.* **1995**, *34*, 1609.
(18) Biasutti, M. A.; Rommens, J.; Vaes, A.; De Feyter, S.; De Schryver, F. D.; Herwig, P.; Müllen, K. *Bull. Soc. Chim. Belg.* **1997**, *106*, 659.
(19) Traficante, D. D.; Nemeth, G. A. *J. Magn Reson.* **1987**, *71*, 237.

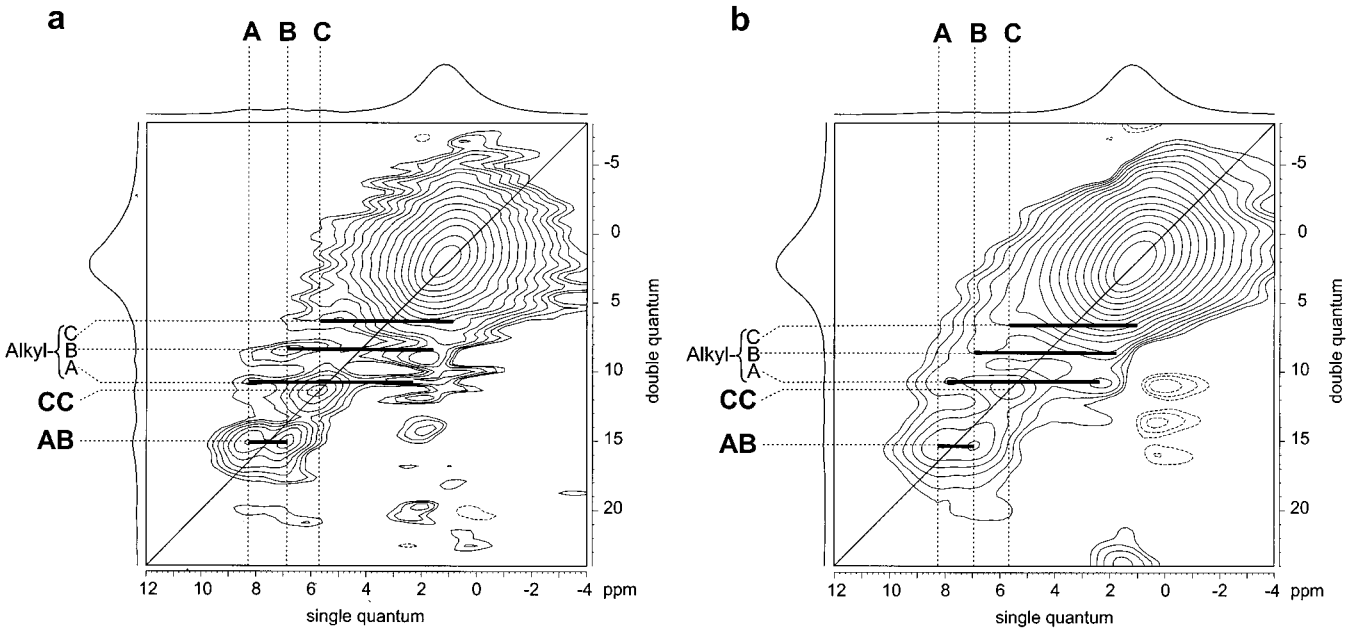

Figure 2. Rotor-synchronized ^{1}H DQ MAS NMR spectra, together with skyline SQ and DQ projections, of (a) α-deuterated and (b) fully protonated HBC-C_{12}, recorded at 35 kHz using one cycle of the BABA recoupling sequence for the excitation and reconversion of DQCs. The assignment of the peaks is discussed in the text.

the crystal, leading to inequivalent aromatic proton sites within each HBC disk, with the axial motion in the LC phase then making the sites equivalent on the NMR time scale. These scenarios can be distinguished by DQ MAS NMR, which we now turn to.

Two-Dimensional Rotor-Synchronized DQ MAS Spectra. Information about the relative proximities of the three resolved aromatic protons is provided by the rotor-synchronized ^{1}H DQ MAS two-dimensional spectrum of α-deuterated HBC-C_{12} in Figure 2a, recorded using one cycle (of duration one rotor period, τ_R) of the BABA[8] recoupling technique for the excitation and reconversion of double-quantum coherences (DQCs). A detailed account of this method and the semiquantitative interpretation of such DQ MAS spectra is given in ref 6.

Here, we focus on the peaks in the bottom left-hand corner of the spectrum, due to DQCs involving only aromatic protons (the top right-hand corner is dominated by the intense signal due to the alkyl chain protons). As is evident from the molecular structure of HBC-C_{12}, the six aromatic protons are grouped in pairs of "bay protons" with a H−H distance of approximately 0.20 nm, while the closest interpair distance is 0.41 nm. Therefore, the aromatic region of the DQ MAS spectrum will be dominated, for the short excitation period[12] used here, by the dipole−dipole couplings within the three pairs. In Figure 2a, it is clear that the extension to a second frequency dimension has yielded a significant resolution improvement over the one-dimensional spectrum (Figure 1a), and the three separate resonances can be clearly distinguished without having to resort to potentially unreliable data processing methods. A strong CC auto peak and AB cross-peaks are observed, which imply the presence of only two types of pairs of aromatic protons, H_A-H_B and H_C-H_C, in a ratio, as determined from the peak intensities, of 2:1. Note that, in such a DQ spectrum, an auto peak arises from a DQC between two dipolar-coupled-like (isochronous) nuclei; in contrast, two *J*-coupled-like nuclei do not give rise to an auto peak in the analogous solution-state INADEQUATE experiment.[1,20] (In Figure 2a, in addition to the CC auto peak and AB cross-peaks, weak cross-peaks due to DQCs between the aromatic protons and undeuterated alkyl protons can also be seen.)

For unsubstituted HBC, an X-ray single-crystal study[21] showed that the molecules pack in the so-called herringbone pattern, which optimizes the $\pi-\pi$ interactions between adjacent disks. We hypothesize here, on the basis of the observed spectral features, that HBC-C_{12} adopts the same columnar packing of the aromatic cores as in unsubstituted HBC, with the presence of the long alkyl chains now meaning that the individual columns of aromatic cores are much more separated from each other. Figure 3 shows how such a stacking of the HBC cores leads to three different aromatic proton environments. Three aromatic cores are shown; the molecules above and below the central aromatic core are indicated by dashed and dotted lines, respectively, with the aromatic protons of the central layer highlighted.

The interplanar distance in unsubstituted HBC is 0.342 nm,[21] and thus the aromatic protons of one layer will additionally experience the ring currents of the extended π-electron systems of adjacent layers. As was demonstrated by Waugh and Fessenden as early as 1956,[22] when a proton sits above an aromatic ring system as in, for example, [10]paracyclophane, it experiences a large shielding effect and hence a marked high-field shift (in this solution-state NMR example, the closed loop structure fixes the position of the central methylene protons above the aromatic ring).

In HBC-C_{12}, three different aromatic proton environments can thus be identified with respect to the degree to which the proton experiences the ring current of the adjacent layers. The unshaded circles represent protons which lie neither above nor below the π orbitals of an adjacent layer and therefore correspond to the least shielded resonance (highest ppm). Fully shaded and hatched circles then represent protons which lie over or below an inner and outer part, respectively, of an adjacent ring system; the fully shaded protons would be expected to be the most shielded. Assigning the unshaded, hatched, and fully

(20) Buddrus, J.; Bauer, H. *Angew. Chem., Int. Ed. Engl.* **1987**, *26*, 625.

(21) Goddard, R.; Haenel, M. W.; Herndon, W. C.; Krüger, C.; Zander, M. *J. Am. Chem. Soc.* **1995**, *117*, 30.

(22) Waugh, J. S.; Fessenden, R. W. *J. Am. Chem. Soc.* **1956**, *79*, 846.

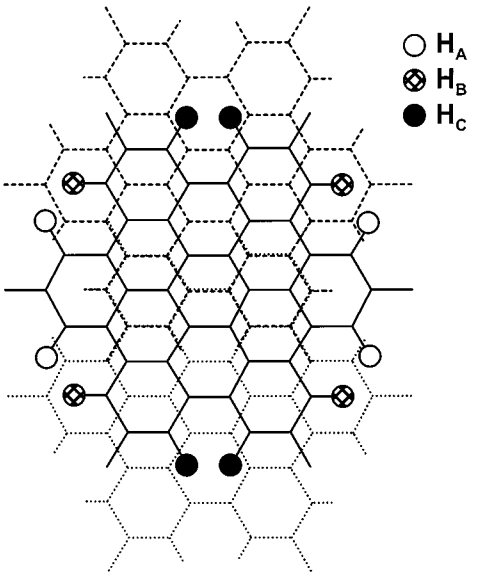

Figure 3. Representation of the proposed stacking of the aromatic cores in HBC-C_{12}, based on the structure of unsubstituted HBC, which is known, from an X-ray single-crystal study,[21] to crystallize in the so-called herringbone pattern. Three HBC-C_{12} molecules are shown; the molecules above and below the central HBC-C_{12} molecule are indicated by dashed and dotted lines, respectively. The labeling of the aromatic protons of the central layer is discussed in the text.

shaded protons to the A, B, and C resonances in Figure 2, respectively, the observed presence of only AB and CC pairs in the ratio 2:1, with the C resonance having the smallest chemical shift value (most shielded), is then explained. Thus, it is the second of the two scenarios, i.e., the reduction of the six-fold to a two-fold symmetry for each individual molecule, identified at the end of the previous section which is borne out by experiment.

For comparison, Figure 2b shows the analogous DQ MAS spectrum for the fully protonated HBC-C_{12}. In this case, although the three aromatic resonances are less well resolved, the presence of only AB and CC pairs in the ratio 2:1 is still clearly apparent in the spectrum. It should also be noted that, in Figure 2b, cross-peaks corresponding to DQCs between aromatic and alkyl protons, which are largely suppressed in Figure 2a on account of the deuteration of the α-carbons, are now of comparable intensity to the aromatic−aromatic peaks.

Although care should be taken with the interpretation of these aromatic−alkyl peaks on account of their existence as only weak shoulders of the intense alkyl auto peak, the following features are noteworthy. First, the cross-peaks involving H_A, which are the best resolved, correspond to DQCs involving alkyl protons with a chemical shift of 2.3 ppm, whereas the intense alkyl auto peak is centered at 1.1 ppm. This observation is, of course, in agreement with what is known from solution-state NMR, namely that the α-methylene protons are shifted to low field relative to the other alkyl protons, which are more removed from the aromatic core. What is more interesting is that the resonances involving the α-methylene protons close to H_B and H_C are apparently shifted to about 1.8 and even 1.0 ppm, respectively. Such an observation is consistent with the fact, as revealed by Figure 3, that the α-methylene protons close to H_B and H_C experience to a greater extent the ring current of the adjacent layers than do the α-methylene protons close to H_A. In this respect, we would like to add that we have observed a clearer demonstration of this effect for a related compound, in which the long alkyl chains are replaced by *tert*-butyl groups, with in this case two distinct methyl resonances (at +1.3 and −0.6 ppm) being resolved.[23] Thus, we observe that both the aromatic and the nearby alkyl protons of HBC disks are subjected to the aromatic ring current of adjacent layers, and the extent of this effect reflects the packing of the molecules.

DQ MAS Spinning Sideband Patterns. For such a system as HBC-C_{12}, which contains well-isolated spin pairs, a quantitative evaluation of the dipolar couplings can be achieved by extending the spectral width in the DQ dimension and then analyzing the observed DQ spinning sideband patterns.[9,10,12,24] The origin of such patterns is of interest, since for an isolated spin pair there is no anisotropic evolution of the DQCs during t_1 (any ^{1}H chemical shift anisotropy effects will be negligible at the very fast ω_R used). Thus, DQ spinning sidebands cannot arise by the normal single-quantum mechanism, whereby the observed sideband pattern can be considered to map out the anisotropy of the spin interaction which is active during the evolution period. Instead, it has been shown that the origin of such spinning sidebands lies in the rotor-encoded change between the Hamiltonian active during the reconversion period and that active during the excitation of DQC.

For an isolated spin pair and using N cycles of the BABA recoupling method for both the excitation and reconversion of DQCs, the DQ time domain signal is given by[12]

$$s(t_1,t_2=0) = \langle \sin[3/(\pi\sqrt{2})D\sin(2\beta)\cos(\gamma+\omega_R t_1)N\tau_R] \times \sin[3/(\pi\sqrt{2})D\sin(2\beta)\cos(\gamma)N\tau_R]\rangle \quad (1)$$

where β and γ are Euler angles relating the principal axes system of the dipolar coupling tensor to the rotor-fixed reference frame, and the brackets denote a powder average. The dipolar coupling constant, D, is defined as

$$D = \frac{(\mu_0/4\pi)\hbar\gamma_H^{\,2}}{r^3} \quad (2)$$

where r is the internuclear distance.

Figure 4a and b presents experimental DQ MAS spinning sideband patterns, together with the best-fit spectra (dotted lines), for the aromatic protons in the crystalline and LC phases of α-deuterated HBC-C_{12}, respectively. The MAS frequency was 35 and 10 kHz in (a) and (b), respectively, with two rotor periods being used for excitation/reconversion in both cases, such that the product $N\tau_R$ equals 57 and 200 μs in the two cases. The chosen excitation/reconversion times ensured the presence of at least significant third-order sidebands, thus improving the sensitivity of the observed pattern to D. The best-fit spectra correspond to the Fourier transformation of DQ time domain data sets generated using eq 1, with the powder average being performed numerically. As is evident from the insets on the right of Figure 4, the DQ spinning sideband patterns are very sensitive to the dipolar coupling constant, D, and the excitation/reconversion time, $N\tau_R$.

For the crystalline phase, the displayed spectrum corresponds to proton H_A (at 8.3 ppm), though essentially the same pattern is obtained for protons H_B and H_C. In addition to the peaks of interest due to the aromatic−aromatic DQCs in (a), further peaks (marked by *) corresponding to DQCs between aromatic and residual undeuterated α-carbon protons are observed. (Note the change in the relative intensity of the peaks due to the two types

(23) Brown, S. P.; Schnell, I.; Brand, J. D.; Müllen, K.; Spiess, H. W. *J. Mol. Struct.* Accepted for publication.

(24) Friedrich, U.; Schnell, I.; Brown, S. P.; Lupulescu, A.; Demco, D. E.; Spiess, H. W. *Mol. Phys.* **1998**, *95*, 1209.

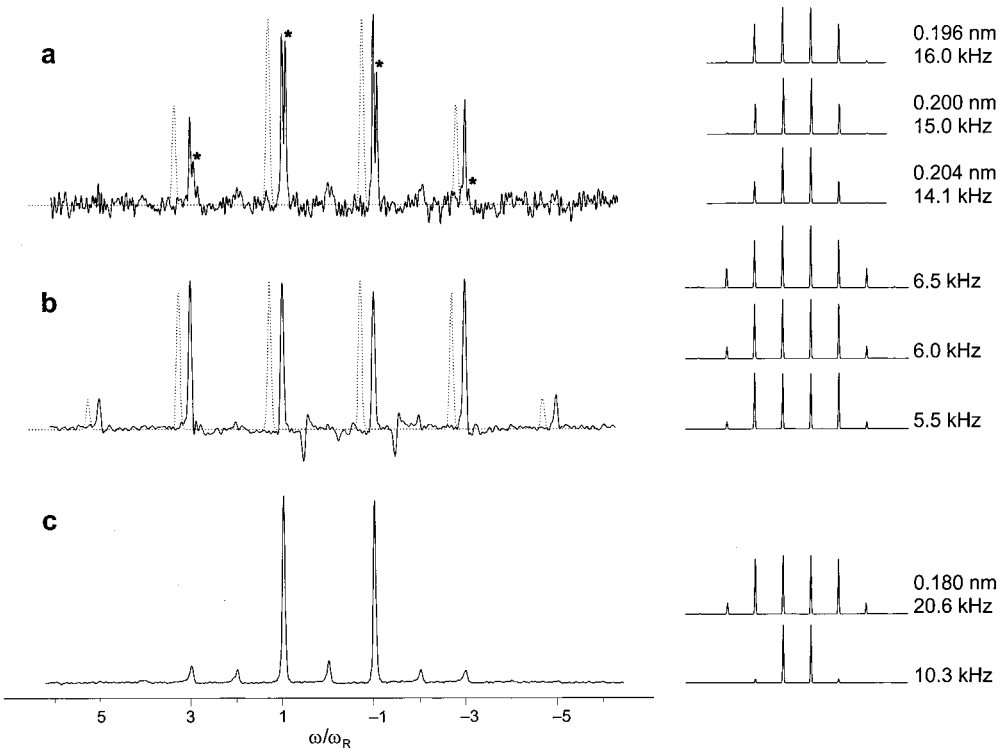

Figure 4. Extracted columns from ^{1}H DQ MAS spectra of α-deuterated HBC-C_{12}, showing the DQ spinning sideband patterns for (a) the aromatic protons at 8.3 ppm and (c) the alkyl protons at 1.2 ppm in the crystalline phase ($T = 333$ K), and (b) the aromatic protons at 6.2 ppm in the LC phase ($T = 386$ K). In each case, best-fit spectra, generated according to the spin-pair expression in eq 1, are shown (shifted to the left to allow a better comparison) as dotted lines. A spinning frequency, $\omega_R/2\pi$, equal to 35 and 10 kHz was used for the crystalline and LC phases, respectively, with the two-rotor-period compensated BABA recoupling sequence (see Experimental Section) being used for the excitation and reconversion of DQCs in both cases. In (a), additional peaks corresponding to DQCs between aromatic and residual undeuterated α-carbon protons are marked by asterisks. The insets to the right of the experimental spectra display simulated spinning sideband patterns for various cases discussed in the text.

of DQCs on increasing the excitation/reconversion time from one (Figure 2a) to two rotor periods (Figure 4a).[12])

For an isolated spin pair, only odd-order DQ spinning sidebands are expected; in real systems, the presence of perturbing spins is often evidenced by the observation of both a centerband and even-order sidebands (the analogous observation of odd-order sidebands in triple-quantum MAS spectra has been discussed in refs 24 and 25). The effective absence of both a centerband and even-order sidebands in Figure 4a,b means that the interpretation of the experimental spectra using the analytical spin-pair theory is appropriate here. The best-fit spectra for the crystalline and LC phases then correspond to dipolar coupling constants, $D/(2\pi)$, equal to 15.0 ± 0.9 and 6.0 ± 0.5 kHz, respectively.

For the crystalline case, the measured D equates to an internuclear distance, r, between the two aromatic protons of 0.200 ± 0.004 nm. The evaluated distance is thus in good agreement with the X-ray single-crystal structure, which predicts such r to be between 0.190 and 0.196 nm.[21] The slightly larger value obtained in this NMR study could provide evidence for small deviations of the C−C−H bond angles from the ideal 120° and/or slight out-of-plane distortions of the C−H bonds.

Comparing the evaluated D values for the crystalline and LC phases, a reduction of D by a factor of 0.40 ± 0.04 is observed. In the LC phase, fast axial rotation of the molecule about an axis perpendicular to the ring (passing through the center of symmetry) is expected.[26] For a molecule undergoing such a motion, the dipolar coupling constant is reduced by a factor of $^1/_2(1 - 3\cos^2\theta)$, where θ is the angle between the principal axes system (here the internuclear vector) and the molecular rotation axis.[2] Thus, for the case where the internuclear vector is perpendicular to the rotation axis ($\theta = 90°$), a reduction by a factor of 0.5 is expected. If there were small out-of-plane distortions of the C−H bonds, this would then lead to a deviation of θ from 90°, and thus a larger reduction; for example, θ equal to 75° would give the experimentally observed value. Alternatively, the value of 0.40 could be explained by postulating the presence of out-of-plane motion in addition to the axial rotation.

It is interesting to compare the observed result with a previous study[16] where, using the same molecule but with the aromatic protons instead of the α-carbon protons deuterated, a reduction of 0.42 in the ^{2}H quadrupolar splitting was observed for the LC phase. Although the small discrepancy of the two results is within the experimental error, it should be remembered that the principal axes systems (PAS) are different in the two cases; for ^{2}H NMR it is the C−H bond direction (in some cases, the principal axes system of the electric field gradient tensor for the ^{2}H quadrupolar coupling may slightly deviate from the C−H bond direction[4]) rather than the H−H internuclear direction which is of interest. Thus, the effect of a motional averaging process will not necessarily be the same.

The effect of the axial motion in the LC phase was also apparent in the one-dimensional spectra (Figure 1), where, as noted earlier, the spectrum changes, upon the phase transition, from containing three distinct resonances to a single line, with a frequency close to the average of the three resonances in the crystalline phase. This means that the axial motion interchanges positions H_A, H_B, and H_C, but importantly the $\pi-\pi$ packing

(25) Friedrich, U.; Schnell, I.; Demco, D. E.; Spiess, H. W. *Chem. Phys. Lett.* **1998**, *285*, 49.

(26) Demus, D., Goodby, J. W., Gray, G. W., Spiess, H. W., Vill, V., Eds.; *Handbook of Liquid Crystals*; Wiley-VCH: Weinheim, 1998.

arrangement in the columnar phase must be very similar to that in the crystalline phase. Indeed, support for this statement is provided by the significant shift to high field of the frequency of the aromatic resonance in the ^{1}H solution-state NMR spectrum on increasing the concentration.

The DQ MAS spinning sideband pattern shown in Figure 4c corresponds to the alkyl protons of α-deuterated HBC in the crystalline phase (the column was extracted from the same two-dimensional spectrum as that from which Figure 4a was obtained). A previous ^{1}H DQ MAS investigation of malonic acid yielded a proton−proton internuclear distance of 0.180 nm for the rigid CH_2 group in a crystalline sample.[10] As shown in the inset, under the excitation conditions used, such a rigid CH_2 group would then give rise to a DQ MAS spinning sideband pattern containing third- and first-order spinning sidebands of approximately equal height. Clearly, the experimental spectrum bears no similarity to such a spectrum and rather corresponds to a dipolar coupling constant, $D/(2\pi)$, equal to 10.3 kHz (compared to 20.6 kHz, which would be expected for a rigid pair with an internuclear distance of 0.18 nm). Thus, the presence of significant motional narrowing for the alkyl chains in the crystalline phase is clearly demonstrated. Such alkyl chain motion was hinted at by the previously presented STM image of a monolayer of HBC-C_{12} adsorbed onto graphite.[17]

Discussion

In this paper, the suitability of very fast MAS ^{1}H NMR methods to the investigation of both the structure and dynamics of an alkyl-substituted hexa-*peri*-hexabenzocoronene, HBC-C_{12}, which forms a columnar mesophase, has been clearly demonstrated. For the crystalline phase, three distinct aromatic resonances were resolved in the single-quantum MAS spectrum. The internuclear proximities of these resolved protons identified by a rotor-synchronized two-dimensional DQ MAS spectrum then proved a reduction of symmetry for each molecule from a six-fold to a two-fold rotation axis. It should be noted that the reliability of this DQ MAS method for such structural investigations has been previously demonstrated for a range of systems, where X-ray single-crystal data are available.[6,10,11,27]

The observed NMR results were rationalized by hypothesizing, for crystalline HBC-C_{12}, a herringbone structure of aromatic cores as in unsubstituted HBC. In this way, the $\pi-\pi$ interactions are particularly pronounced, with the packing resembling that formed by the carbon layers in graphite, and the observation of the distinct aromatic resonances could then be explained in terms of the differing degrees to which the aromatic protons experience the ring current of adjacent layers. Although it is well known in solution-state NMR, to the best of our knowledge this represents the first clear demonstration in the solid state of this phenomenon.

An alternative explanation for the observation of three aromatic resonances would be a reduction from six- to two-fold symmetry arising as a consequence of a conformational distortion of either the aromatic core or the alkyl chains. For example, a reduction to a two-fold symmetry, due to a preferential orientation of the alkyl chains parallel to one of the three main axes of the underlying graphite axes, was observed in the STM image of a monolayer of HBC-C_{12} adsorbed onto graphite.[17] However, it is most unlikely that the very wide range of aromatic shifts (5.6−8.3 ppm) and, in particular, the pronounced high-field shift of the C resonance (at 5.6 ppm) observed in the NMR spectra could arise from a conformational distortion, and instead all the evidence strongly supports the ring current hypothesis. Furthermore, in a follow-up study,[23] we have investigated the crystalline phase of hexa-*tert*-butyl-substituted HBC, where a single crystal suitable for an X-ray structure determination could be prepared. In this case, the more complicated ^{1}H DQ MAS spectrum was found to be very well explained on the basis of the known structure, invoking the same arguments involving the exposure of protons to ring currents hypothesised here.

The suitability of NMR to the investigation of variable-temperature phenomena meant that the changes which occur in the ^{1}H NMR spectra upon the transformation from the crystalline to LC phase could be easily followed. In the one-dimensional spectrum, the axial motion in the LC phase leads to an averaging of the three aromatic proton resonances into a single resonance, but with a frequency which indicates that the $\pi-\pi$ packing largely persists. Moreover, the analysis of DQ MAS spinning sideband patterns meant that it was possible to quantify the reduction of the dipolar coupling due to motion in the LC phase. By comparison to the value which was determined for the crystalline phase, where the corresponding internuclear distance between the aromatic protons was shown to be in good agreement with the X-ray structure of unsubstituted HBC, a reduction by a factor of 0.40 was observed. Additionally, again on the basis of an analysis of the DQ MAS spinning-sideband pattern, significant mobility of the alkyl chains in the crystalline phase could be identified.

In a previous study,[6] we have shown the applicability of the ^{1}H DQ MAS method to the investigation of hydrogen bonding, where it was emphasized that the method has the advantages of requiring neither the preparation of a single crystal nor isotopic labeling, as well as being quick in terms of the required experimental time, on account of the excellent sensitivity of ^{1}H NMR. For the HBC-C_{12} sample studied in this paper, it proved impossible to prepare a single crystal, presumably because of the mobility of the alkyl chains discussed above; thus, the applicability of NMR to powdered samples meant that ^{1}H DQ MAS spectroscopy could deliver information which was not available from scattering methods. Moreover, this NMR method is also applicable to only partially ordered systems, such as liquid crystals, and amorphous glassy systems.[28] The acquisition of rotor-synchronized ^{1}H DQ MAS spectra, which provide such valuable information about proton−proton proximities, was again quick, with the presented spectra requiring an experimental time of only 26 min (Figure 2a). It should be noted that the acquisition of DQ MAS spinning sideband patterns required significantly longer experimental times (8 h).

We have also successfully applied the DQ MAS method to a range of other (fully protonated) alkyl-substituted HBC samples, in which some or all of the long alkyl chains are replaced by, for example, isopropyl or *tert*-butyl groups.[23] Thus, high-resolution solid-state ^{1}H single- and double-quantum MAS NMR offers itself as a highly promising tool for the study of, e.g., packing effects in new materials which exploit $\pi-\pi$ interactions for optical and optoelectronic applications.

Experimental Section

Synthesis of α-Deuterated HBC-C_{12} (1). The synthesis is outlined in Scheme 1. As the first step, 4-bromododecanophenone (**3**) was coupled with trimethylsilylacetylene to yield **4**. After cleavage of the trimethylsilyl group, the resulting acetylene derivative **5** was coupled with **3** to obtain the tolane **6**. The latter was converted to **7** by a cobalt

(27) Dollase, W. A.; Feike, M.; Förster, H.; Schaller, T.; Schnell, I.; Sebald, A.; Steuernagel, S. *J. Am. Chem. Soc.* **1997**, *119*, 3807.

(28) Feike, M.; Jäger, C.; Spiess, H. W. *J. Non-Cryst. Solids* **1998**, *223*, 200.

Scheme 1

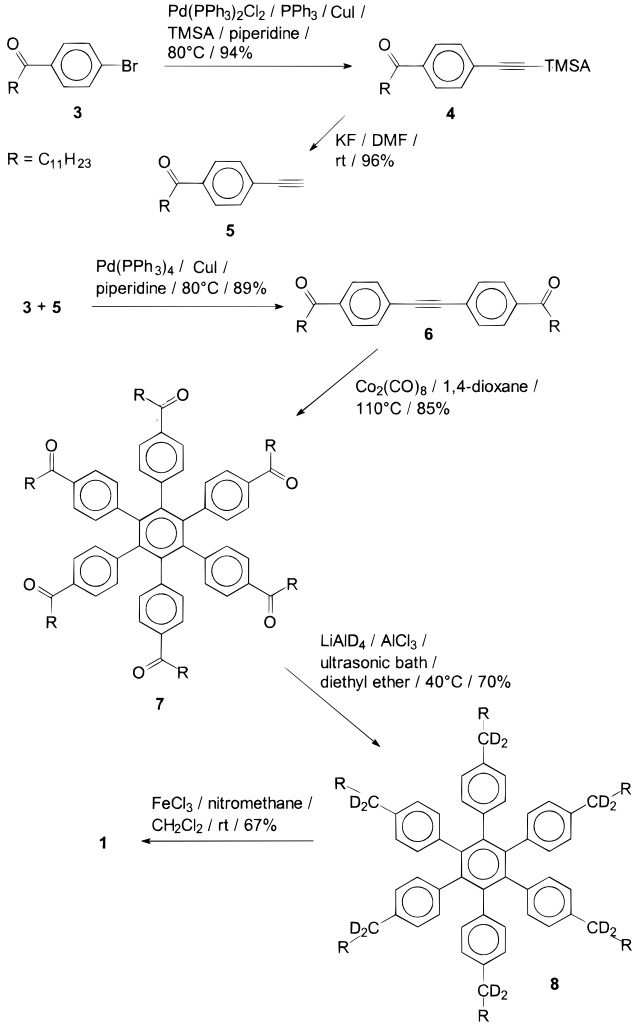

octacarbonyl-catalyzed cyclotrimerization. The introduction of deuterium was then achieved by a very efficient reduction of the keto group using lithium aluminum deuteride in the presence of aluminum chloride[29]—in a modification of the original process, it was here found necessary to treat the refluxing reaction mixture with ultrasound. A small amount of olefinic side product was removed by a subsequent hydrogenation using hydrogen in the presence of a palladium/charcoal catalyst. The cyclodehydrogenation of **8** to yield the title compound **1** was achieved with anhydrous iron(III) chloride/nitromethane in dichloromethane.

Synthesis of α-Protonated HBC-C_{12} (2). A synthesis of **2** is described in ref 16; in this work, the same route was followed up to the nondeuterated analogue of the hexaphenylbenzene derivative **8**. However, it was found that the cyclodehydrogenation to yield the title compound **2** could be performed more reproducibly by the same anhydrous iron(III) chloride/nitromethane in dichloromethane method as was used in the synthesis of **1**: To a stirred solution of hexakis(4-dodecylphen-1-yl)benzene (5.0 g, 3.24 mmol) in dry CH_2Cl_2 (700 mL) was added a solution of $FeCl_3$ (anhydrous) (17 g, 104.8 mmol) in dry nitromethane (200 mL). An argon stream was bubbled through the reaction mixture throughout the entire reaction. After being stirred for 30 min at room temperature, the reaction was quenched with methanol (1000 mL), and the precipitate was filtered. After being dried under vacuum, the residue was chromatographed on silica gel, first with petroleum ether and toluene to remove side products, and then with hot toluene to elute the yellow band of the product. Recrystallization first from toluene and then from heptane yielded 3.8 g (77%). $K_1 \rightarrow K_2$, 315 K [285 K], 21 kJ/mol; $K_2 \rightarrow \mathrm{Col_{ho}}$, 380 K [355 K], 92 kJ/mol. The melting point (380 K) was observed to be significantly higher than that previously reported,[16] indicating a greater degree of purity of the final product for the modified synthetic route described here.

NMR. ^{1}H MAS NMR experiments were performed on a Bruker ASX 500 spectrometer at a ^{1}H Larmor frequency of 500.1 MHz, using a double-resonance MAS probe supporting rotors of outer diameter 2.5 mm with a spinning frequency of up to 35 kHz. At these very fast spinning frequencies, the additional heating effect caused by air friction becomes significant. Using the ^{119}Sn resonance of $Sm_2Sn_2O_7$ as a chemical shift thermometer, the correction term relative to the bearing gas temperature has been calibrated in a separate study.[30] All stated temperatures have been corrected by this procedure. For all samples, the 90° pulse length was 2.0 μs, and a recycle delay of 3 s was used. For one-dimensional MAS experiments, 16 transients were averaged. In addition, a solution-state ^{1}H NMR spectrum of the α-deuterated HBC-C_{12} dissolved in deuterated chloroform was recorded on a Bruker DMX 500 spectrometer at the same ^{1}H Larmor frequency (500.1 MHz).

DQ MAS experiments were performed using the back-to-back (BABA) recoupling sequence[8] for the excitation ($p = 0 \rightarrow p = \pm 2$, where p is the coherence order) and reconversion ($p = \pm 2 \rightarrow p = 0$) of DQCs. (For rotor-synchronized experiments, the standard sequence, $P_x-\tau-P_{-x}-P_y-\tau-P_{-y}$, where τ equals $\tau_R/2$ minus the pulse durations, was used. For the experiments recorded with the aim of observing full DQ MAS spinning sideband patterns, a compensated two-rotor-period variant of the sequence was used:[31] $P_x-\tau-P_x-P_y-\tau-P_{-y}-P_x-\tau-P_x-P_{-y}-\tau-P_y$.) A final 90° pulse was used to create transverse magnetization, with the duration of the $p = 0$ "z-filter" period set equal to one rotor period. The total phase cycle[32] used consisted of 16 steps with four steps to select $p = \pm 2$ after the excitation sequence and four steps to select $p = 0 \rightarrow p = -1$. Sign discrimination was restored in the F_1 dimension by the TPPI[33] method of incrementing the phase of the excitation pulses by 45°. In the rotor-synchronized experiments, the increment in t_1 was set equal to one rotor period, with, for each of 32 increments, 16 (Figure 2a) and 32 (Figure 2b) transients being averaged. To obtain the DQ MAS spinning sideband patterns, 618 increments of 1.0 and 286 increments of 4.0 μs (corresponding to F_1 spectral widths of 500 and 125 kHz) were used for the crystalline (Figure 4a,c) and LC phases (Figure 4b), respectively, averaging over 16 and 32 transients in the two cases. In the contour plots, solid and dashed lines represent positive and negative contours, respectively, with the bottom contour corresponding to 2.0 and 1.4% of the maximum intensity in Figure 2a and b, respectively, and subsequent contours corresponding to a multiplicative increment of 1.3.

Acknowledgment. S.P.B. thanks the Alexander von Humboldt-Stiftung for the award of a research fellowship. Financial support from the Deutsche Forschungsgemeinschaft, SFB 262, is acknowledged. We thank Dr. Manfred Wagner for recording the solution-state NMR spectrum of HBC-C_{12} (Figure 1d) and, together with Andreas Fechtenkötter, for carrying out the investigation of the concentration dependence of the solution-state aromatic chemical shift. Helpful discussions with Christoph Kayser are acknowledged.

Supporting Information Available: Detailed experimental account of the synthesis of **1**, together with characterization information, including the assignment of the solution-state ^{1}H NMR spectrum of **1** (Figure 1d) (PDF). This material is available free of charge via the Internet at http://pubs.acs.org.

JA990637M

(29) Nystrom, R. F.; Berger, C. R. A. *J. Am. Chem. Soc.* **1958**, *80*, 2896.

(30) Langer, B.; Schnell, I.; Spiess, H. W.; Grimmer, A.-R. *J. Magn. Reson.* **1999**, *138*, 182.

(31) Feike, M.; Demco, D. E.; Graf, R.; Gottwald, J.; Hafner, S.; Spiess, H. W. *J. Magn. Reson.* **1996**, *A122*, 214.

(32) Bodenhausen, G.; Kogler, H.; Ernst, R. R. *J. Magn. Reson.* **1984**, *58*, 370.

(33) Marion, D.; Wüthrich, K. *Biochem. Biophys. Res. Commun.* **1983**, *113*, 967.